ELSEVIER

Ceramics International 33 (2007) 255–261

CERAMICS INTERNATIONAL

www.elsevier.com/locate/ceramint

Influence of ZrO_2 on the thermo-mechanical response of nano-ZTA

D. Sarkar [a,*], S. Adak [a], M.C. Chu [b], S.J. Cho [b], N.K. Mitra [c]

[a] *Department of Ceramic Engineering, National Institute of Technology, Rourkela-8, Orissa, India*
[b] *Division of Chemical Metrology and Materials Evaluation, KRISS 305-600, Republic of Korea*
[c] *Department of Chemical Technology, University of Calcutta, 92 APC Road, Kolkata-9, India*

Received 30 May 2005; received in revised form 9 June 2005; accepted 12 September 2005
Available online 27 December 2005

Abstract

Zirconia dispersed alumina powders have been synthesized in homogenous condition by following the wet interaction process at varying ZrO_2 content and the thermo-mechanical behavior of the same has been studied. The tetragonal phase is retained at room temperature without any deliberate addition of stabilizer, which has been explained on the basis of particle size effect in terms of lower surface energy of the t-phase compensating for the difference in chemical free energy. Flexural strength follows an inverse relation with temperature due to reduction of driving force for t → m transformation. The toughness and strength reduce significantly above 10 mol.% ZrO_2 beyond which comparatively large grain growth is observed. The thermal expansion hysteresis associated with t → m transformation is evident with martensitic temperature influenced by ZrO_2 content and grain size.

Keywords: B. Grain size; B. Nanocomposites; C. Thermal shock resistance; D. ZrO_2

1. Introduction

Alumina has very high hardness and good strength but relatively low toughness in comparison to zirconia, which exhibits very high strength and good toughness but shows relatively poor hardness. The strength and toughness of alumina may be enhanced by dispersion of zirconia solid solutions, mainly due to the tetragonal–monoclinic transformation [1–4]. In Al_2O_3 matrix, t-ZrO_2 grains undergo the t → m transformation (stress-induced phase transformation), and microcracks form around existing m-ZrO_2 grains (microcrack formation) [5–7]. Thus, toughness of Al_2O_3-ZrO_2 composites is improved by both stress-induced phase transformation toughening and microcrack toughening of dispersed zirconia. Additionally, the increase in t-ZrO_2 grain size enhances the ability to trigger the transformation during fracture and hence the transformation toughening mechanism predominates [8,9]. Wolten first suggests that this t → m phase transformation is martensitic in nature, which follows an athermal and diffusionless behavior with a thermal hystersis and shear-type mechanism [10]. The martensitic start temperature (M_s) increases with increase in the grain size of the tetragonal zirconia-phase precipitates [11]. It also depends on the grain size distribution of zirconia [12,13]. Thus, fracture toughness of ZrO_2 doped alumina composites is controlled and optimized by the amount of ZrO_2 content and its grain size. On the other hand, the reduction in grain size to the nanoscale level is advantageous over the coarse grained materials to improve the strength and hardness [14]. However, the reduction in Young's modulus of nanocomposites is reported by others to be the result of level of porosity and state of cracks in the samples [15]. The mechanical properties of ZTA ceramics are closely related to different thermal properties; mainly thermal coefficient. Moreover, thermal shock resistance is directly related to maximum stress, thermal conductivity and coefficient of thermal expansion.

In order to account for the temperature changes during processing and characterization, the thermal expansion coefficients of alumina and zirconia are an important parameter, in which the latter being higher than the former. This differential expansion contributes to a tensile stress that reduces slightly the compressive stress on the ZrO_2 when quenched to room temperature. Therefore, the thermo-mechanical properties of composite material are mainly attributed by the dispersed phase content and grain size. Hence, optimization of amount and size of zirconia on thermo-mechanical properties of nano-ZTA are

* Corresponding author. Tel.: +91 661 2462207; fax: +91 661 2462999.
E-mail address: dsarkar@nitrkl.ac.in (D. Sarkar).

0272-8842/$32.00
doi:10.1016/j.ceramint.2005.09.012

Table 1
Important parameters of powders and sintered composites

Batch no.	Code	Al_2O_3 (mol.%)	ZrO_2 (mol.%)	Starting powder (nm)	Sintered specimen (1550 °C/4 h)				Relative density (%) (1550 °C/4 h)	Flexural strength (MPa) (25 °C)	K_{IC} (MPa $m^{0.5}$)	H_V (GPa)	E (GPa)
					t-ZrO_2 (%)	m-ZrO_2 (%)	Grain size (μm)						
							Al_2O_3	ZrO_2					
1	A5Z	95	5	20–150	100	0	0.2–0.8	0.08–0.15	98.22	521	5.31	16.83	305
2	A75Z	92.5	7.5	30–180	98	2	0.2–0.7	0.08–0.17	98.06	607	6.24	15.86	293
3	A10Z	90	10	20–160	91	9	0.15–0.6	0.07–0.2	97.42	721	6.84	15.21	286
4	A15Z	85	15	25–170	88	12	0.15–0.5	0.09–0.25	96.62	636	6.41	14.98	267

studied systematically in the present work. The paper also discusses the influence of zirconia content and grain size in Al_2O_3-x mol.% ZrO_2 (where $x = 5, 7.5, 10, 15$) with regard to the transformation effects.

2. Experimental procedure

ZTA composites were prepared in the range of 5–15 mol.% ZrO_2. The starting powders were processed by sol–gel route [16]. The batch composition and particle sizes were shown in Table 1. The powders were pressed uniaxially (30 MPa) and isostatically (300 MPa) prior to subsequent sintering in muffle furnace at different temperature ranging from 1450 to 1550 °C with an interval of 50 °C at different time schedule. Crystalline phases present in the sintered billets were identified by X-ray diffractometer (Cu Kα, PHILIPS PW-1830) technique. The sintered density of billets (4 mm × 3 mm × 40 mm) was measured by immersion in kerosene using Archimedes' principle.

The elastic modulus (E) was measured using an ultrasonic tester employing the pulse-echo technique. Fracture toughness and hardness were measured on the polished surface by Vicker's indentation method in accordance with Anstis formula [17]. The reported values were the average of data obtained from five indentation tests. Flexural strength was determined by standard 4-pt bending method in an instrument with a 30 mm outer span and 10 mm inner span and cross head speed of 0.5 mm min^{-1}. Fractographs were studied by SEM (JEOL-JSM840) and the average grain sizes were determined from the microstructure using line intercept method. The retention of metastable t-ZrO_2 and thermodynamically stable m-ZrO_2 phase was ascertained for both the polished and fractured surfaces in regard to Garvie's method [18].

Thermal shock resistance of the samples was studied as resistance to weaken or fracture under stresses generated due to temperature fluctuations. Billets of 4 mm × 3 mm × 40 mm dimension were heated in an electric furnace from 200 to 1200 °C with an interval of 200 °C and soaked for 30 min. Subsequently, heated bars were quenched in water at room temperature, kept for 10 min followed by sudden reheating at corresponding tested temperatures for 10 min. This cycle was repeated twice and the retained flexural strength was measured by Instron 4465. Three samples were taken to determine the retained flexural strength at each test and the average values have been reported here. Thermal expansion measurements were conducted in the temperature range from room temperature to 1400 °C at heating and cooling rate of 5 °C min^{-1} in dilatometer (Netzsch DIL 402C) using high-grade quartz as reference.

3. Results and discussions

3.1. Densification

The powder compacts were sintered at 1450–1550 °C with different dwell times. Relative densities of the sintered materials, plotted against zirconia content at different time and temperatures, are shown in Fig. 1. The reported values are the average of data obtained from five specimens. At 1450 °C, the relative density decreases from 75 to 72% with the addition of ZrO_2 and also exhibits low densification. The rate of densification increases beyond 1500 °C and good densification is achieved at 1550 °C. The maximum density of ~98% ρ_{th} can be achieved with addition of 5 mol.% ZrO_2 at 1550 °C for 4 h. However, for higher ZrO_2 content (15 mol.%), a density as high as ~96% ρ_{th} is achieved at 1550 °C (Table 1 and Fig. 1). This is caused by the lowering of t-ZrO_2 phase at higher content of ZrO_2 [19]. The decrease in t-ZrO_2 phase or simultaneous

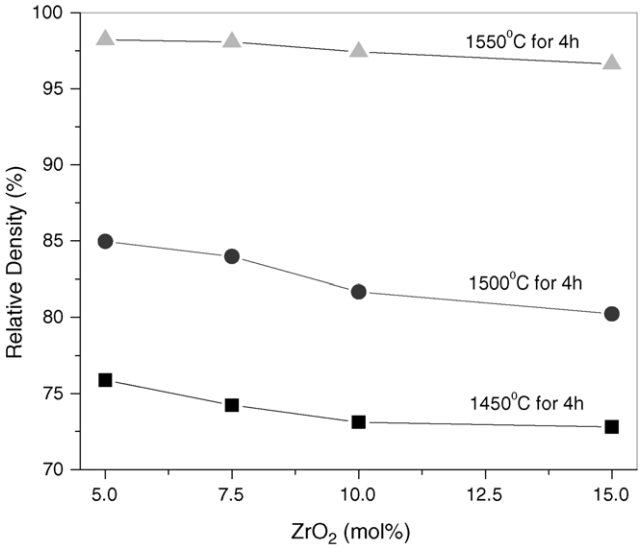

Fig. 1. Relative density at different temperatures with Al_2O_3 composites at varying ZrO_2 content.

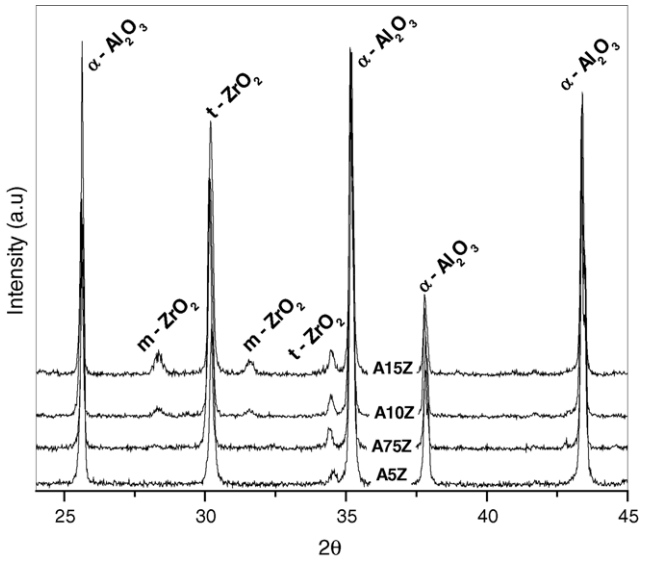

Fig. 2. XRD of polished Al_2O_3-x ZrO_2 (where $x = 5$, 7.5, 10, 15 mol.%) composites sintered at 1550 °C/4 h.

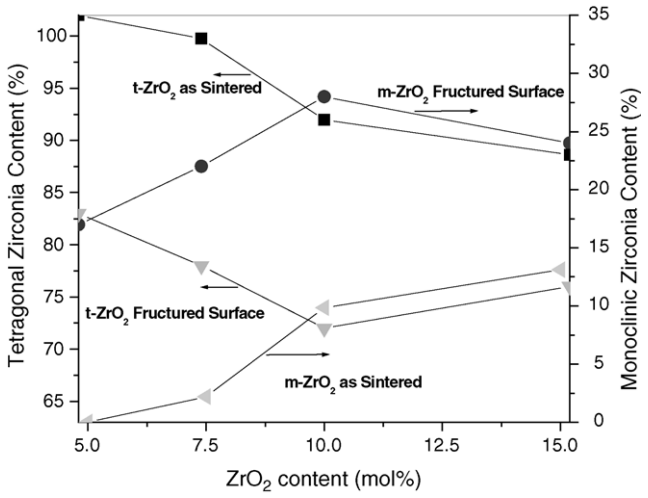

Fig. 3. t-ZrO_2 and m-ZrO_2 content of polished and fractured surfaces as a function of ZrO_2.

increase in m-ZrO_2 phase may be explained by a rapid increase in grain size of zirconia particles. However, the very fast grain growth rate has a detrimental effect on the density in final stage sintering of A15Z, since pore coalescence in alumina matrix and segregation of zirconia particles takes place [20].

3.2. Microstructure and phase content

The XRD patterns of ZTA ceramics after sintering at 1550 °C for 4 h are shown in Fig. 2, which demonstrates the difference of content phases. The XRD patterns of ZTA ceramics containing 5–7.5 mol.% ZrO_2 are almost the same. The ZrO_2 particles are mainly of tetragonal phase embedded in α-Al_2O_3. The main peaks of t-ZrO_2 are sharp and high. The A10Z and A15Z samples contain t-ZrO_2 phase over 90 and 85%, respectively, which reveals their good stability. The m-ZrO_2 phase increases with increasing ZrO_2 content and 12% m-ZrO_2 phase can be detected in composites containing 15 mol.% ZrO_2 (Table 1). The variation of t-ZrO_2 fraction in sintered and fractured specimens is given in Fig. 3. The retention of t-ZrO_2 varies during fracture and t-ZrO_2 fraction decreases with increasing zirconia content. However, t-ZrO_2 retention becomes much easier to trigger the transformation to monoclinic. As a result, its contribution to transformation toughening predominates. However, fracture toughness value reduces abruptly when zirconia grain size is over a critical size [21] and the ease of transformation inhibited above the critical size.

Fig. 4 shows the fractography of as sintered materials. Average alumina grain (gray contrast) sizes are 0.5 and 0.3 μm for A5Z and A15Z, respectively, are fairly homogeneous in each composite. ZrO_2 grains (white contrast) are homogeneously distributed throughout the Al_2O_3 matrix with a typical particle size, $d_{average}$ [ZrO_2], from 120 nm in A5Z to more than 200 nm in A15Z. The present study shows that ZrO_2 grains are located at alumina triple points. In the A5Z material more than one of every two triple points is occupied by zirconia particles, two of every three triple points are filled with zirconia particles in A75Z and zirconia particles are present in nearly all triple points for both A10Z and A15Z composites. The addition of zirconia is very effective in hindering the grain growth of alumina during sintering, even for the lowest zirconia content. The addition of up to 10 mol.% ZrO_2 prevents grain growth without allowing the formation of zirconia agglomerates, which are very deleterious for the mechanical stability of the composite. However, the premature zirconia agglomeration can be observed in case of composites containing 15 mol.% ZrO_2. Fig. 5 exhibits that the increase in ZrO_2 content increases ZrO_2 grain size as well as decreases grain size of Al_2O_3.

3.3. Mechanical properties

3.3.1. Hardness and elastic modulus

Hardness and elastic modulus of the studied materials may be explained on the basis of porosity and the grain size. Vickers Hardness and elastic modulus of sinter samples at different concentration of zirconia are shown in Fig. 6. The hardness of the ZTA composite decreases (17–15 GPa) with the addition of zirconia as alumina is harder than zirconia. Higher amount of zirconia has an adverse affect on the hardness of the composites due to coarsening of the zirconia grains and formation of subsequent porosity. It has been noticed that these composite materials also obey Hall–Petch relationship [22–24]. The present study shows that the average particle size has significant impact on hardness value, which is controlled by particle size.

Elastic modulus of the composite depends on the volume fraction of the phases present and their individual modulus of elasticities. At 1550 °C densification of the composites is improved by reducing pore volume fraction of the matrix (Fig. 1) and as a result of which the modulus of elasticity improves. Alumina has a higher modulus of elasticity compared

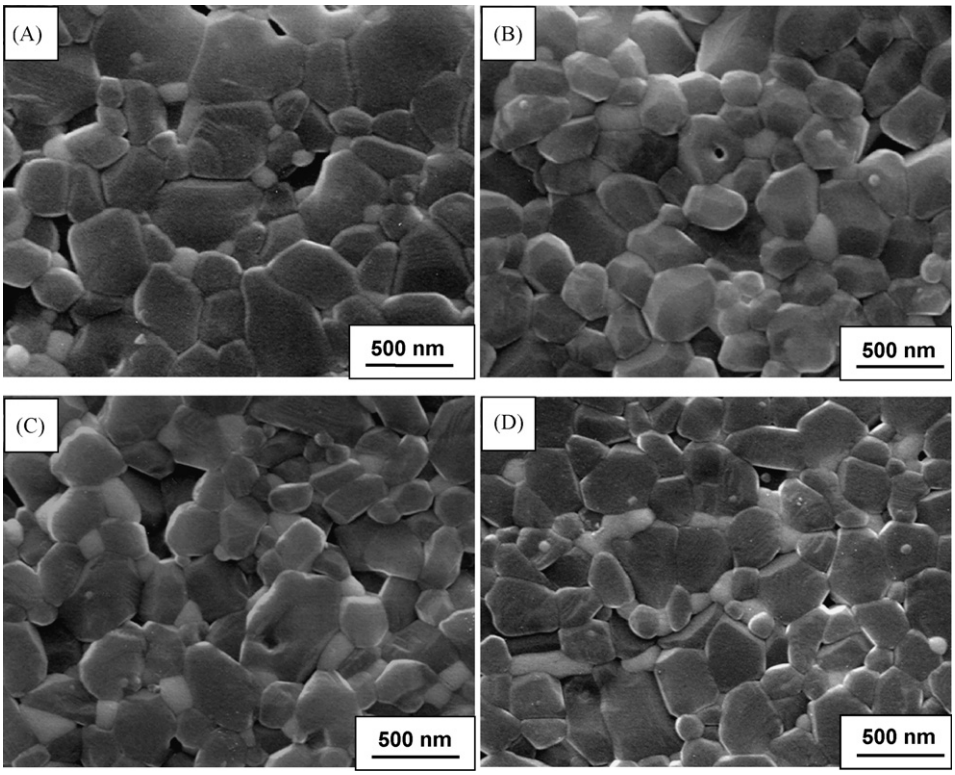

Fig. 4. SEM microstructure of fracture surface of Al_2O_3–ZrO_2 composite sintered at 1550 °C for 4 h, represented as A5Z (A), A75Z (B), A10Z (C), A15Z (D). The phases with gray and white contrast indicate Al_2O_3 and ZrO_2, respectively. The black irregular shape represents the corresponding pores in the sintered body.

to zirconia. So, samples containing 5 mol.% zirconia have the highest modulus of elasticity whereas specimen containing 15 mol.% zirconia has lower levels of densification at a given sintering temperature compared to other samples having lower amount of zirconia. Simultaneously, the grain sizes of zirconia increase and hinder the grain growth of alumina at 1550 °C, which contributes to the lowering of elastic modulus.

Lange [25] reported that both Young's modulus and hardness of ZTA composites containing particles of zirconia stabilized with 2 mol.% Y_2O_3 followed a linear rule of mixtures. A typical Vickers indentation at 49 N load on the polished surface of A10Z composite is shown in Fig. 7. The sign of noticeable plastic deformation around the Vickers indentation zone is absent and the length of radial cracks emanating from the indentation corners is measured in order to evaluate the indentation toughness, a parameter indicative of the resistance to crack propagation. Despite measuring high hardness, the fracture toughness improves with respect to

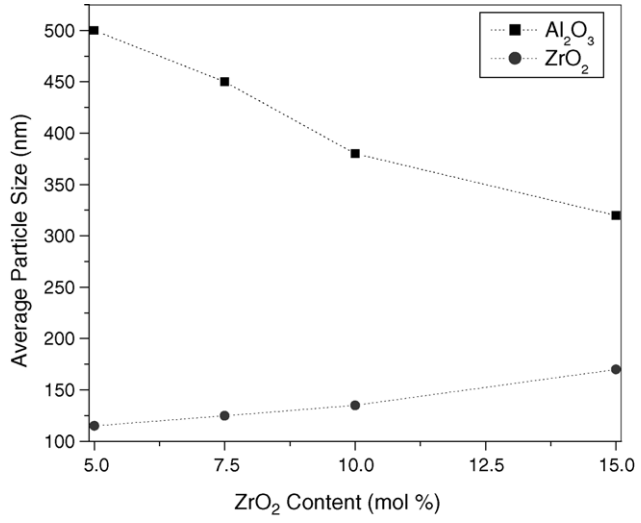

Fig. 5. Average particle size of alumina and zirconia of ZTA composite as the function of ZrO_2.

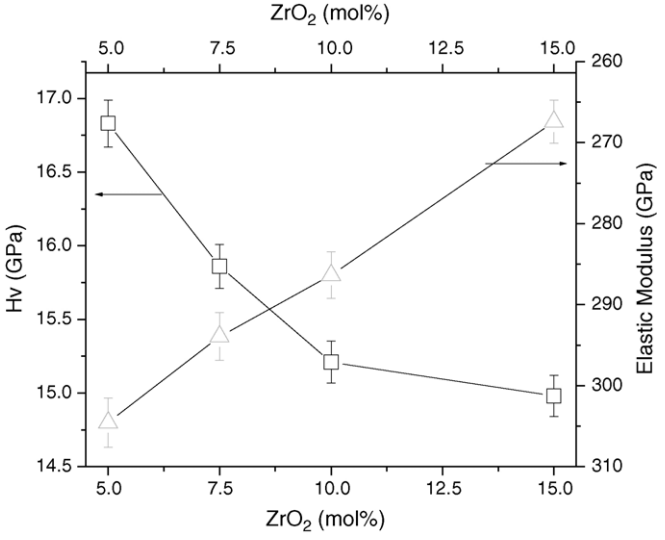

Fig. 6. Elastic modulus and Vickers hardness (at 5 kg load) as a function of zirconia content.

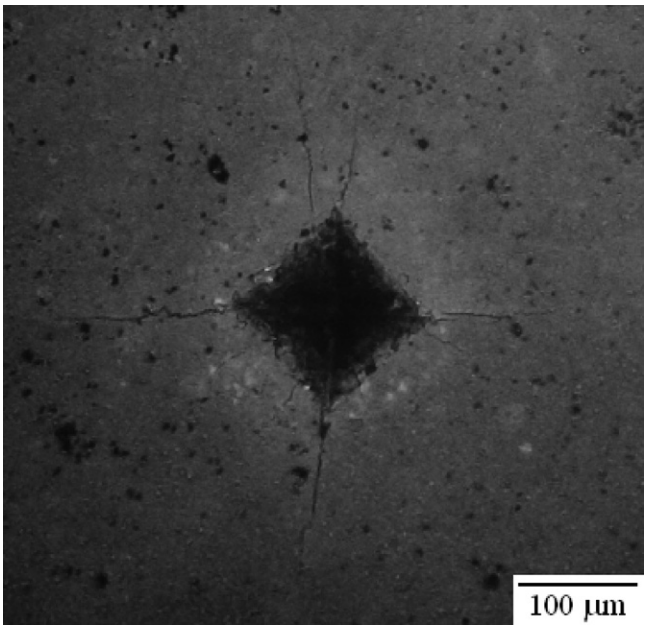

Fig. 7. The Vickers indentation (at 5 kg indent load) on the A10Z ceramic and the propagation of the radial cracks.

pure alumina to a value of around 7 MPa $m^{1/2}$. The higher hardness can be correlated with the observation of finer grain size in the sintered materials.

3.3.2. Fracture toughness and strength

In the present study, the zirconia grain size increases linearly with increasing zirconia content. The fracture toughness and fracture strength of ZTA composite at different zirconia content are reported in Fig. 8. The fracture toughness as well as fracture strength increases linearly with increasing grain size because the tetragonal zirconia grains do not undergo the stress-induced transformation to the monoclinic form when grain size is smaller than a critical size. The particle size lower than the critical value do not affect the strength during fracture test. The reduction of size improves the bulk density but not the transformability of the tetragonal zirconia grains. Usually, the effect of grain size on toughness and strength in transformation-toughened ceramics is a complex phenomenon. An increase in grain size improves the transformability (i.e., tetragonal to monoclinic), therefore increasing toughness and strength. Depending on grain size, the spontaneous tetragonal to monoclinic transformation occurs in ZTA ceramics during cooling from the sintering temperature, leading to degradation in the mechanical properties. The phase transformation behavior can be explained by X-ray diffraction of the sintered materials (Fig. 2) and fracture surfaces (Fig. 3). In sintered specimens, the monoclinic form increases with the addition of zirconia, whereas under stress, the amount of monoclinic phase of fractured surface decreases under stress for the composite containing ZrO_2 more than 10 mol.%. The presence of large fraction of m-ZrO_2 in A15Z is responsible for the strength degradation because it has been recognized that the increase in volume and shear strains accompanied by $t \rightarrow m$ phase transformation invariably cause microcracking.

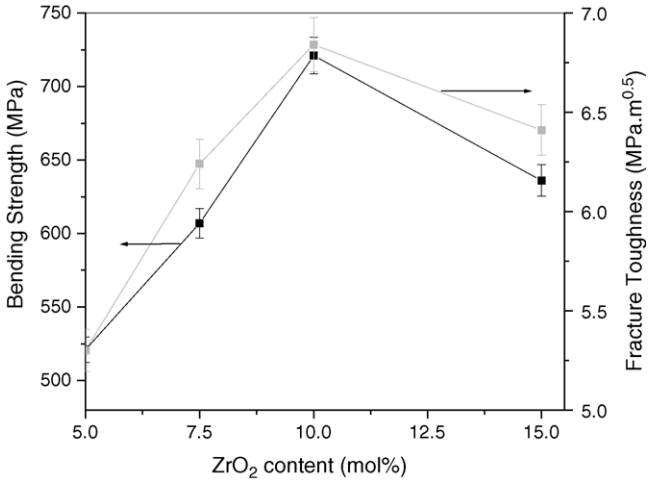

Fig. 8. Bending strength and fracture toughness of ZTA composite as a function of ZrO_2.

3.4. Thermal properties

3.4.1. Thermal shock resistance

The thermal shock resistance of ZTA nanocomposites fabricated from the sol–gel precursor powder is investigated by a water-quenching method. Fig. 9 shows the relative dependence of residual strength of the samples on the temperature difference of thermal shock. A rapid decrease in retained strength occurs around a critical temperature difference (ΔT_c) below which the original strength is retained. The strength reduces more gradually with further increase in ΔT.

The dispersion of ZrO_2 increases the critical temperature difference (ΔT_c) of Al_2O_3, though the overall strength reduces significantly above 10 mol.% addition of ZrO_2. This behavior in ΔT_c can be discussed with the variations in mechanical and

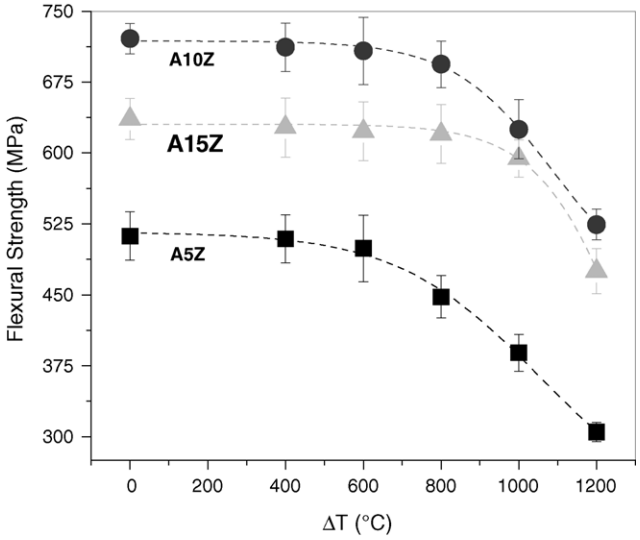

Fig. 9. Plot of retained flexural strength vs. thermal shock temperature for Al_2O_3 with variation of ZrO_2.

thermal properties of the ZrO_2 dispersed ZTA composites as well as temperature difference dependence of the surface heat transfer coefficient at the water–ceramic interface during quenching. The fracture initiated through thermal shock has been given by [26]:

$$\Delta T_c = \frac{\sigma_f(1-\gamma)}{E\alpha\beta} \quad \text{and} \quad \beta = \frac{h_t x}{\lambda}$$

where ΔT_c is the critical temperature difference, σ_f the flexural strength, γ the Poisson's ration, E the modulus of elasticity, α the thermal expansion coefficient, h_t the heat transfer coefficient, λ the thermal conductivity, x the characteristic dimension.

A minimum temperature difference ΔT_c is required to initiate fracture. Below ΔT_c no change in crack length and/or strength is observed. Usually the fracture is initiated and strength decreases at ΔT_c. As the temperature difference of thermal shock increases beyond ΔT_c, crack growth occurs quasi-statically with decrease in strength. The decrease in retained strength up to 600 °C (ΔT) is marginal except in case of 5 mol.% zirconia. Retained strength of 5 mol.% zirconia reduces to about 40% of its original strength when quenched in water from 1200 °C. A10Z and A15Z composites lose their strength on quenching in water from 800 to 1000 °C, respectively. Based on the zirconia content, the retained strength varies from 25 to 40% in case of A10Z and A5Z, respectively. The lowest retained strength is observed in case of 5 mol.% ZrO_2 samples. Critical temperature difference ΔT_c is in between 600 and 1000 °C for A10Z. For Y-TZP/Al_2O_3 materials the drop in flexural strength is more than 50% at 1000 °C [27].

Thermal-stress-induced cracks dissipate their crack tip energy through stress-induced phase transformation. It is expected that the crack propagates along the grain boundaries and finally loose the energy to propagate while moving inside the grain. Therefore, stress-induced phase transformation of monoclinic to tetragonal zirconia absorbs the energy of the crack tip thus arresting its propagation. The phase transformation of tetragonal to monoclinic zirconia reduces with increase in temperature. This is probably due to the reduction in differential free energy between the tetragonal and monoclinic phase. The disappearance of phase transformation strengthening and reduction in Young's modulus contributes to the lowering of flexural strength at elevated temperature. In addition, thermal mismatch between two surfaces also enhances stresses and reduces mechanical properties beyond addition of 10 mol.% ZrO_2.

3.4.2. Thermal expansion behavior

Since the thermally activated and stress-induced reversible tetragonal to monoclinic transformation is always associated with 4–5% dilatation strain, a dilatometer study serves as an excellent tool in studying such transformations. In the starting material, the high temperature stable tetragonal phase is retained at room temperature during rapid cooling after sintering, and remains metastable in the microstructure of the nano zirconia dispersed alumina composite. The slope of the thermal expansion curve is basically the thermal expansion coefficient (α), and any appreciable change in slope can indicate a phase transition. To understand this phenomenon, the dilatational measurement was carried out on the sintered materials (A10Z and A15Z) in the temperature range from room temperature (RT) to 1450 °C (Fig. 10). The expansion in volume occurs linearly with temperature during heating and coefficient of thermal expansion in A10Z can be encountered within the range of 8×10^{-6} to $9 \times 10^{-6}\,K^{-1}$ at 1000 °C. However, the phase transformation during heating and cooling are different and consequently two curves are not identical until they coincide at temperature forming a thermal hysteresis loop. From the dilatation curve, it is proposed that the M_s temperature of A15Z begins to alter at higher temperature compared to A10Z, because of larger inclusion size of ZrO_2 in A15Z.

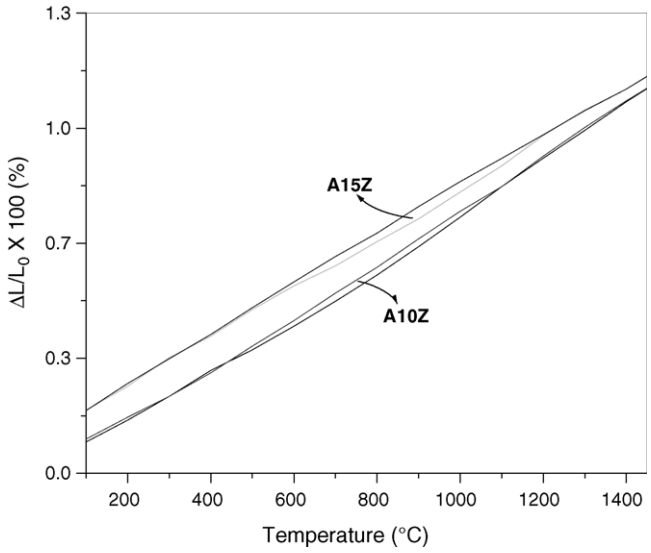

Fig. 10. Thermal expansion curve of Al_2O_3-x ZrO_2 (where $x = 10$ and 15 mol.%) sintered at 1550 °C/4 h.

4. Conclusions

Zirconia toughened alumina nano-composite with 98% relative density has been achieved at 1550 °C. For homogenous dispersion of ZrO_2 in Al_2O_3, the optimum amount of ZrO_2 was found to be 10 mol.% and up to this critical amount of ZrO_2 addition, flexural strength and fracture toughness increase and the size of the intergranular zirconia strongly influences these particles. Similarly, the elastic modulus and hardness follows inverse relationship with ZrO_2 content. The hystersis effect in the dilation curve due to $t \rightarrow m$ transformation is also influenced by the grain size of ZrO_2.

References

[1] S. Hori, M. Yoshimura, S. Somiya, Strength-toughness relations in sintered and isostatically hot pressed ZrO_2-toughened Al_2O_3, J. Am. Ceram. Soc. 69 (3) (1986) 169–172.
[2] S. Hori, R. Kurita, M. Yoshimura, S. Somiya, Suppressed grain growth in final stage sintering of Al_2O_3 with dispersed ZrO_2 particles, J. Mater. Sci. Lett. 4 (9) (1985) 1067–1070.

[3] S. Hori, M. Yoshimura, S. Somiya, R. Takahashi, Al2O3-ZrO2 ceramics prepared from CVD powders, in: N. Claussen, M. Ruhle, A.H. Heuer (Eds.), Advances in Ceramics, vol. 12, Science and Technology of Zirconia II, The American Ceramic Society, Columbus, Ohio, 1984 , pp. 794–805.
[4] G.L. Messing, M. Kumangi, Low-temperature sintering of seeded sol–gel-derived, ZrO_2-toughened Al_2O_3 composites, J. Am. Ceram. Soc. 72 (1) (1989) 40–44.
[5] K. Tsukuma, K. Ueda, M. Shimda, Strength and fracture toughness of hot isostatic-pressed Y_2O_3-partially stabilized ZrO_2/Al_2O_3 composites, J. Am. Ceram. Soc. 68 (1) (1985) C-4.
[6] V.V. Srdic, L. Radonjic, Transformation toughening in sol–gel-derived alumina-zirconia composites, J. Am. Ceram. Soc. 80 (8) (1997) 2056–2060.
[7] B. Lawn, Fracture of Brittle Solids, second ed., Cambridge Solid State Science Series, Cambridge University Press, Oxford, UK, 1993.
[8] A.H. Heuer, N. Clausen, W.M. Kriven, M. Rühle, Stability of tetragonal ZrO_2 particles in ceramics matrices, J. Am. Ceram. Soc. 65 (12) (1982) 642–650.
[9] D.J. Green, Critical microstructures for microcracking in Al_2O_3-ZrO_2 composites, J. Am. Ceram. Soc. 65 (12) (1982) 610–614.
[10] G.M. Wolten, J. Am. Ceram. Soc. 46 (1963) 418.
[11] J. Wang, M. Rainforth, R. Stevens, The grain size dependence of the mechanical properties in TZP ceramics, Br. Ceram. Trans. J. 88 (1989) 1–6.
[12] M.V. Swain, Grain-size dependence of toughness and transformability of 2 mol.% Y-TZP, J. Mater. Sci. Lett. 5 (1986) 1159–1162.
[13] P.F. Becher, M.V. Swain, Grain size-dependent transformation behavior in polycrystalline tetragonal zirconia ceramics, J. Am. Ceram. Soc. 20 (1992) 1178–1184.
[14] H. Gletter, Prog. Mater. Sci. 33 (1989) 223–315.
[15] G.W. Nieman, J.R. weertman, R.W. Siegel, J. Mater. Res. 6 (1991) 1012–1027.
[16] D. Sarkar, S. Adak, N.K. Mitra, Preparation and characterization of Al_2O_3-ZrO_2 nanocomposite, Part I: Powder Synthesis and Transformation Behavior during Fracture, Compos. Part A: Appl. Sci. Manufac., accepted 2005.
[17] G.R. Anstis, P. Chantikul, B.R. Lawn, D.B. Marshall, A critical evaluation of indentation techniques for measuring fracture toughness: I. Direct crack measurements, J. Am. Cer. Soc. 64 (1981) 533.
[18] R.C. Garvie, P.S. Nicholson, Phase analysis in zirconia systems, J. Am. Ceram. Soc. 55 (1972) 303–305.
[19] L.B. Garrido, E.F. Aglietti, Reaction-sintered mullite–zirconia composites by colloidal processing of alumina–zircon–CeO_2 mixtures, Mater. Sci. Eng. A369 (2004) 250–257.
[20] F. Cambier, C. Baudin de La lastra, P. Pilate, A. Leriche, Br. Ceram. Trans. J. 83 (1984) 196.
[21] P.F. Becher, K.B. Alexander, A. Bleirer, S.B. Waters, W.H. Warwick, Influence of ZrO_2 grain size and content on the transformation response in the Al_2O_3-ZrO_2 (12 mol.% CeO_2) system, J. Am. Ceram. Soc. 76 (3) (1993) 657–663.
[22] E.O. Hall, Proc. Phys. Soc. (Lond.) B64 (1951) 747–753.
[23] N.J. Petch, J. Iron Steel Inst. 174 (1953) 25–28.
[24] C. Suryanarayana, Nanocrystalline materials, Int. Mater. Rev. 40 (2) (1995) 41.
[25] F.F. Lange, Transformation toughening. Part 4. Fabrication, fracture strength and toughness of Al_2O_3-ZrO_2 composites, J. Mater. Sci. 17 (1982) 225.
[26] D.P.H. Hasselman, Unified theory of thermal shock fracture initiation and crack propagation in brittle ceramics, J. Am. Ceram. Soc. 52 (1969) 600–604.
[27] D.J. Green, Transformation toughening and grain size control in β''-Al_2O_3/ZrO_2 composites, J. Mater. Sci. 20 (7) (1985) 2639–2646.